Testing an Indium Matching Layer for Acoustic Transducers

Emily Mann

I. Abstract

Searching for the Dark Matter particle (a mysterious material that composes nearly 85% of the matter in the universe) is a very exciting endeavor for physicists. The PICO Collaboration is currently conducting a direct detection experiment that uses a bubble chamber filled with superheated liquid that is sensitive to nuclear recoils. Bubbles will form when energy deposits cause a phase change in the liquid. These interactions are monitored by sound and video equipment. Before a sound wave, caused by the formation of a bubble within the detector, comes in contact with an acoustic transducer, it has three mediums (the superheated liquid, the inner fused silica quartz vessel and the Lead Zirconate Titanate (PZT) piezoelectric transducer) that it must pass through. When there is a difference in acoustic impedances in two materials, some of the sound will be reflected. It is supposed to be possible to minimize this difference by creating an intermediate layer with acoustic impedance between that of the two materials. In previous attempts, a matching layer made of MAS epoxy and tungsten carbide powder has been used to create an appropriate acoustic impedance [1], but this matching layer dampened the signal. Here we attempt to use a shim of pure indium instead. This paper describes the development of an acoustic matching layer to be implemented on acoustic devices on the PICO Collaboration dark matter detectors.

II. Dark Matter

It has been found [2] that nearly 85% of the matter in the universe is not composed of the normal, baryonic matter seen every day, but rather, is made up of exotic particles that form what has come to be known as Dark Matter [2]. Dark Matter does not interact with light and the particles that make up this substance have never been directly detected, on Earth or by satellite. Even though astronomical observations show the existence of Dark Matter, experiments must be conducted to prove the hypothesis that it is an exotic elementary particle. There are many experiments that search for Dark Matter in the universe either directly by looking for nuclei scattered by Dark Matter particles, or indirectly by detecting by products of Dark Matter annihilation.

III. Observational Evidence

The existence of dark matter is apparent when one observes its gravitational effects on large systems in the universe. The first person to hypothesize dark matter was Jan Oort in 1932 [3]. He used dark matter to explain the orbital velocities of stars in the Milky Way galaxy, but did not give it a specific name nor did he assign properties to the missing mass. A year later, Fritz Zwicky advanced this idea by using two different techniques while observing the Coma Galaxy cluster. Zwicky first derived the mass of the cluster using the Virial theorem [1], which relates the average over time of the kinetic energies in a system to the total potential energy of the system as a function of its mass. He also used a technique called the mass-luminosity relationship to derive the mass of the cluster. This relation uses an understanding of how many atoms are incorporated into the stars within a galaxy as well as the fraction of atoms in a cluster, which are in individual galaxies, and an understanding of the luminosity of stars in relation to their mass. Zwicky calculated the system's mass using the virial theorem and found it to be nearly 500 [1] times (later calculated to be about 40 times) greater than the mass calculated using the mass-luminosity relation. This drastic difference led Zwicky to postulate the existence of a large amount of unseen mass. He called this mass "dunkel materie", or dark matter.

In the 1970s, Vera Rubin was studying the rotational speed of spiral galaxies when she found that the predicted angular motion of the Andromeda galaxy (Fig. 1) and its actual motion had some large discrepancies—this was later proven to be true for many other spiral galaxies [3].

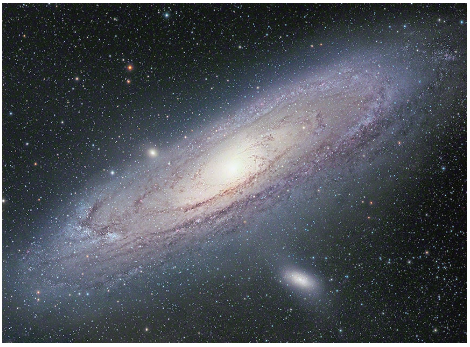

Figure 1. The spiraled Andromeda galaxy
http://www.guidescope.net/galaxies/andromeda.htm

Using an image tube spectrograph and the Mt. Wilson 100 inch telescope, Rubin and Kent Ford were able to measure the velocities of individual regions of the Andromeda galaxy. Over two years, they observed and recorded the velocities of 67 [3] regions within Andromeda. The results puzzled researchers. Rubin and Ford found that objects around the outside of the galaxy were traveling with the same velocity as those near the center (Fig 2).

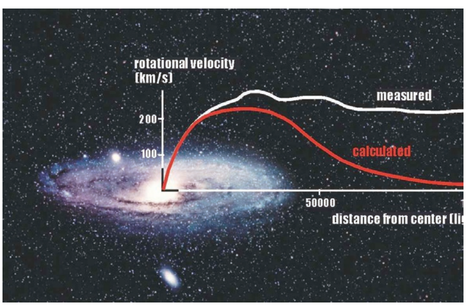

Fig 2. Calculated rotational velocities vs. those observed by Vera Rubin and Kent Ford
http://cdms.phy.queensu.ca/Public_Docs/Pictures/Rotationcurve_3.jpg

This is counter-intuitive since Newton's laws of motions and gravity dictate that as the distance from the center of a mass increases, the velocity should decrease. The fact that the spiral arms of galaxies were observed to have uniform velocities regardless of distance from the center of visible mass of that galaxy supports the claim that there is unaccounted mass in these galaxies [4].

Other evidence for the existence of dark matter in the universe comes from gravitational lensing—the visible effect gravity has on light rays in the universe. This technique gives scientists a method of observing objects that do not interact with light but still have mass[6]. Some other evidence for dark matter comes from the early universe and Big Bang Nucleosynthesis [7].

IV. Searches for Dark Matter

Observations have helped physicists narrow down candidates for dark matter particles. One early candidate for the dark matter particle was the neutrino—a weakly interacting subatomic particle. These non-baryonic particles make up "hot" dark matter, due to their small mass and, as a direct result of this, high velocity comparable to that of the speed of light [8]. While these particles interact the way dark matter particles could, their high speeds make it a very unlikely candidate. If all of the missing matter were hot neutrinos, the distribution of density in the universe would be much smoother than what has been observed [9]. To properly explain the observed distribution of mass in the universe, the dark matter particle must be electrically neutral, have a small velocity, and interact, at most, via the weak force.

Another hypothesis for the dark matter particle that arises from advanced theories of the strong nuclear force is a candidate called the axion. Axions are bosons that would be created "cold" with a small speed, have a non-relativistic population that could account for dark mass, are nearly collision-less, and have very weak couplings with nuclei. These are all properties that would make them good candidates for the dark matter particle [8,9]. The Axion Dark Matter eXperiment (ADMX) has been designed to detect dark matter axions coming from the sun. Using strong magnetic fields, the detector would convert the axion into two photons [10].

The researchers behind ADMX claim to have 90% accuracy in discriminating between normal interactions and axion-photon couplings, yet the ADMX detector has yet to record evidence of axions converting into photons [10].

While there are many candidates that seem to fulfill all the necessary constraints for the dark matter particle, physicist's most favored candidate is a theoretical particle inspired by supersymmetry called a neutralino. These Weakly Interacting Massive Particles (WIMPs) are particles outside of the standard model of particle physics and, if the lightest of these particles are neutral and radioactively stable, they could have the correct relic density to match the quantities of dark matter observed in the universe. WIMPs have a large mass and move at a slow velocity compared to the speed of light, causing interactions with other particles to be rare, but detectable [9].

V. Methods of Detecting Dark Matter

The methods of detecting dark matter can be placed into three categories: indirect detection, creation, and direct detection. Generally, indirect detection searches for by-products of WIMP-WIMP annihilations. The by-products from these are detected either on Earth or in satellites in low Earth orbit. Some of the main indirect detection experiments that have been conducted over the last several years include; the EGRET (Energetic Gamma Ray Experiment

Telescope) gamma ray telescope at the Compton Gamma Ray Observatory [11], the PAMELA (a Payload for Anti Matter Exploration and Light-nuclei Astrophysics) experiment [12], and the Alpha Magnetic Spectrometer—a detector attached to the International Space Station that has previously made headlines with promising reports of what is either pulsars (strongly magnetized neutron stars) or evidence of dark matter [13].

The production technique searches for dark matter particles created in the Large Hadron Collider in Geneva, Switzerland. This is done by colliding particles (such as protons) at extremely high energies, simulating particle interactions during the Big Bang [13]. The signature of Dark Matter at the LHC would involve events with large unbalanced momentum in the plane perpendicular to the beam. Currently, no evidence for Dark Matter has been found at the Large Hadron Collider [14].

The direct detection method looks for dark matter particle interactions with the nuclei of a detector. There are many direct detection experiments and, so far, none of them have yielded indisputable proof for the detection of individual dark matter particles. The PICO experiment uses bubble chambers to search for direct evidence of WIMPS bumping into nuclei of a liquid, which then transforms the liquid into a gas bubble [15].

VI. PICO and Bubble Chambers

The PICO bubble chamber uses a superheated liquid with favorable interaction probability with WIMP candidates [15]. The liquid is contained in a pressure vessel with cameras that observe the interactions. Liquids are considered superheated when they have a temperature greater than the boiling point of the liquid at that pressure without any bubble nucleation occurring. This is only possible with a liquid that is relatively clear of any foreign materials that could trigger spontaneous bubble formation. Because of this, when an outside particle enters the chamber and interacts with a nucleus of the superheated liquid, it triggers a phase change (as the inner chamber liquid is highly sensitive to dense energy deposits created by the recoiling ionized nucleus) (Fig.3). The liquids that are currently employed within the inner vessel are iodotrifluoromethane or CF_3I, and octafluoropropane or C_3F_8 [16]. CF_3I contains iodine, sensitive to spin-independent interactions, and fluorine, which is sensitive to spin-dependent interactions. The advantage of C_3F_8 is that one can see lower energy WIMPS than with CF_3I and it is more chemically stable. These highly sensitive target nuclei make both liquids a good choice for an inner vessel target.

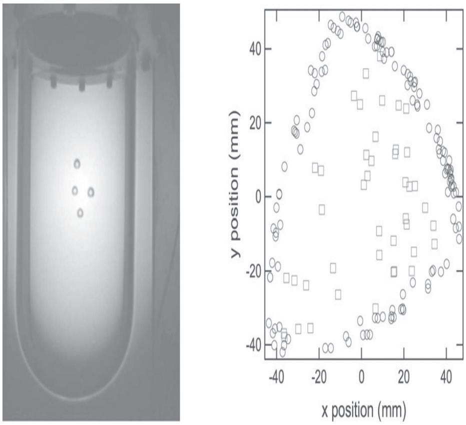

Figure 3. Left: a neutron from a calibrating source scatters off of four nuclei, causing four bubbles to grow. Right: a reconstruction of several of the locations of many neutron calibration events on the x-y plane, the z-axis is in the vertical direction. The graph appears more triangular because of the positioning of the cameras and the fact that some optical effects have not been taken into account. (http://iopscience.iop.org/1742-6596/39/1/027/pdf/1742-6596_39_1_027.pdf)

When a bubble begins to form, it will locally block light and cameras that are driven by software detect the change in pixels. The bubble also emits sound waves [17, 18] and these are recorded on highly sensitive piezoelectric microphones. These microphones are designed and created by the Astroparticle Physics group at Indiana University South Bend. The loudness of the bubble aids in determining what is an interaction with a WIMP and what is background radiation [17, 18]. Currently, the PICO collaboration has successfully completed a dark matter search in the 2L detector filled with C_3F_8 and a 30L vessel filled with CF_3I. Background seen in previous chambers has been successfully reduced and the larger vessel shows increased sensitivity to both spin-dependent and spin-independent WIMPs [19]. The purpose of this project is to test an idea to improve the sensitivity of the sound sensors to the acoustic emissions from the bubbles.

VII. Sound Wave Interactions

When a sound wave comes into contact with a material or medium, a few different interactions occur. All materials have characteristic acoustic impedance, Z, which is a function $Z = \rho V_s$, where V_s is the speed of sound through a material and ρ is the density of the material. Acoustic attenuation will result in a dampening of acoustic sound, but is caused by an actual energy loss due to viscosity in the material. Some of the sound is reflected when passing from one medium to another. The amount of reflection can be calculated using the materials' acoustic impedances [20]. It is possible to minimize reflection by sending sound waves through materials of similar acoustic impedance.

VIII. Piezo Electric Materials and Transducer Improvements

An acoustic transducer is a device that takes acoustic sound and converts it into electrical signals. This is accomplished, in our device, with the use of a piezoelectric crystal (piezo). Piezos, when experiencing pressure, will create dipoles that generate electrical potential. It is now understood that originally isotropic polycrystalline ceramic materials can function as piezos when polarized by a strong electric field [21]. For our acoustic transducers, the piezos are composed of Lead Zirconate Titanate (PZT), which is a robust material.

These PZT acoustic transducers aid the PICO Collaboration in discriminating between alpha particle interactions, neutron interactions, and actual WIMP interactions. When an acoustic signal is received by the piezo and an electric signal is generated, the induced voltage can be recorded and graphed. It was discovered that the amplitude of the sound waves emitted by a bubble nucleation formed by alpha decay of an atom was, on average, higher than those formed by neutron events [17, 18]. The ability to discriminate between events is a vital discovery and it would help to improve discrimination abilities. We are testing the hypothesis that an intermediate layer, composed of pure indium with acoustic impedance between that of the quartz vessel and the piezo, will cause less loss of sound due to signal reflection, making discrimination between events more accurate. It would also reduce the number of transducers used on the chamber, which could minimize alpha interactions, as the piezos are a source of background radiation. To select an appropriate material we need to know the density and speed of sound of candidate materials since $Z=\rho V_s$

IX. Procedure

Measuring the speed of sound through materials

To measure the speed of sound in materials, we placed samples of the material between two transducers; the lower one emits a sound wave and the upper one is used to receive the signal. An oscilloscope that can make high-resolution measurements was used to record the signals.

Fig 4. 148.5 mm sample of copper being measured using this method. The thickness of the sample divided by the time it takes sound to go through it is the speed of sound in the material.

It takes a small amount of time for the signal to leave the emitting piezo, enter the receiver and show a voltage across the receiving piezo. The total amount of extra time from these effects is an offset (t_0). To accurately measure t_0, two transducers were placed together using Glacier FM grease (piezo to piezo) and electrical pulses were sent through a function generator to an amplifier and into the emitter (lower) piezo. The signal was then received by the second piezo connected to the oscilloscope. A distinct "cut off" point was found where the sound was received by the other piezo. We must subtract this t_0 from the times measured when sending signals through material.

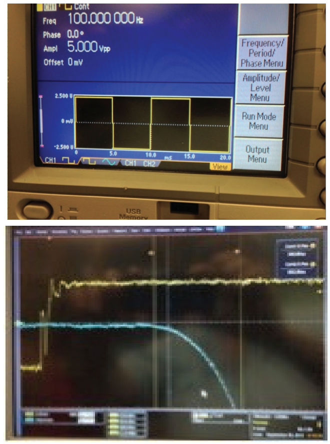

Fig 5. Top: Function generator set to run a pulse at 100 Hz with amplitude of 5V peak to peak, generating a square wave. Bottom: Oscilloscope display showing the time between the signal leaving the first piezo and being received by the second when no sample is introduced. This time difference of 0.34986 μs is then subtracted from measurements taken when a sample was inserted between the piezos.

We next sandwiched rods of material in which the speed of sound is well understood (such as copper) and measured the sound velocity using this technique to see how well our apparatus works. The results are summarized in Table 1.

Sample	Thickness (mm)	Time Difference (us)	Known Speed of Sound (m/s) [21]	Measured Speed of Sound (m/s)	% Difference
No Sample	0	0.34986±0.5 (t_0)			
Copper Bar	52.756±0.001	11.11±0.5	4600	4902.8909±220.6522	6.178
Copper Bar	148.490±0.001	31.63±0.5	4600	4747.0497±75.0403	3.097
Glass	9.6012±0.001	2.12±1	5968	5423.9769±2558.4797	3.9
Tungsten Carbide Bar	103.77±0.001	15.83±0.5	6655	6638.7269±209.6882	0.245

Table 1. Speed of sound measurements through certain material

We then measured the speeound through a thin piece of glass to determine the value of Z needed to the shim. As seen in Table 1, the propagated error on to measured time delay from the pulse traveling through the system glass (1 us as opposed to 0.5 us) is higher than the other materials; this is because the cut off point displayed on the oscilloscope was less obvious than that of the other materials. An error propagation of 1 μs was given to the glass.

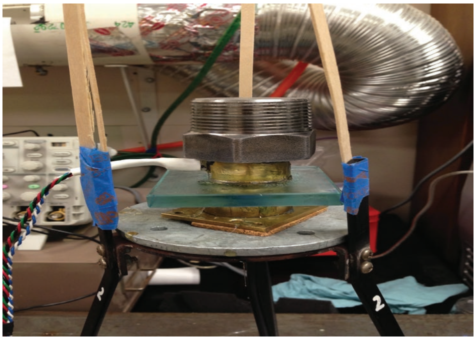

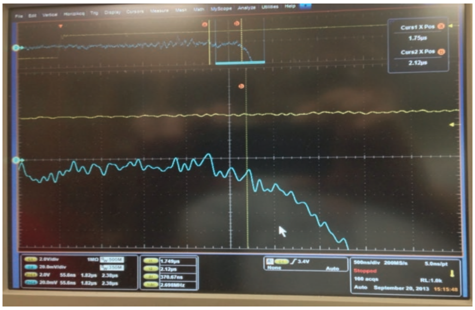

Fig 6. Top: Speed of sound through a thin slab of glass being tested. Bottom: Signal displayed on oscilloscope—it must be noted that the cut off point is less obvious than other samples.

X. Current Tests and Redesign

It was concluded that MAS epoxy and tungsten carbide mixture will only ever impede the flow of acoustic noise. Indium is a malleable metal with a low melting point and an ideal acoustic impedance of ~16 MRayls. This value is between that of the PZT transducers and the fused silica quartz used for the chamber. Because of this, it has been chosen as a good candidate for an intermediate layer.

XI. Measurements to Confirm Indium Pureness

Two, 8 oz ingots of indium were purchased from a private supplier. In order to confirm that the samples were 99.9% pure indium, several measurements were taken.

Mass

Each ingot was weighed individually on a scale in order to confirm, with relative certainty, the seller's claim that each ingot is 8 oz.

Table 2. Ingot Masses

Item	Claimed Mass (g)	Actual Mass (g)	% Difference
Ingot 1	226.7	225 ± 1	0.70%
Ingot 2	226.7	226 ± 1	0.30%

Density

Three different methods of directly measuring density were used to confirm the pureness of the indium

Table 3. Individual Water Displacement

Item	Mass (g)	Volume (cc)	Known Density (g/cc)	Measured Density (g/cc)	% Difference
Ingot 1	225 ± 1	32 ± 1	7.31	7.03 ± 0.22	4%
Ingot 2	226 ± 1	34 ± 1	7.31	6.62 ± 0.22	10%

Table 4. Combined Water Displacement

Item	Mass (g)	Volume (cc)	Known Density (g/cc)	Measured Density (g/cc)	% Difference
Combined Ingots	452 ± 1	64 ± 1	7.31	7.1 ± 0.11	3%

Table 5. Direct Measurement and Calculation

Item	Height (mm)	Average Diameter (mm)	Radius (mm)	Volume (cm^3)	Known Density (g/cm^3)	Measured Density (g/cm^3)	% Difference
Ingot 1	12.49 ± 0.01	56.80 ± 0.01	28.40 ± 0.01	31.60 ± 0.01	7.31	7.12 ± 0.03	2.60%
Ingot 2	12.62 ± 0.01	56.29 ± 0.01	28.15 ± 0.01	31.40 ± 0.01	7.31	7.20 ± 0.03	1.50%

Measured Speed of Sound through an Indium Bar

In order to measure the time it takes for a pulse to pass through a 79 mm indium bar, it was placed between a transducer that sent out the pulse and a transducer that received it. Two separate measurements give the following values:

Table 6. Speed of sound through indium

Measured SOS (m/s)	Known SOS[24] (m/s)	% Difference
2413.11±3.67	2220	8.00%
2416.79±3.70	2220	8.70%

It is important to note that the first value measured for the speed of sound was done by the usual method as described earlier in this paper. The second value was found in a similar method, but using a largely amplified 125 kHz sine wave. These are promising results, as two slightly different methods yield incredibly similar sound velocity measurements. Taking the average of these two to be the actual speed of a signal traveling through indium to be 2414.95 m/s. This gives an acoustic impedance of 17.7 MRayls; this is the value I will use for the remainder of my calculations.

While these measurement techniques yield limited accuracy, it was determined that the samples are 99.9% pure indium.

XII. Melting the Ingots

The ingots were melted down so that the metal could be formed into a long, thin rod that is necessary for acoustic measurements and a flat disc to act as an intermediate layer. To melt the ingots, they were placed into a small ceramic crucible and placed into the oven at 450 degrees Fahrenheit. The glass test tube the metal was to be poured into and the metal stand were also placed in the oven to avoid heat shocking the glass. It took ~20 minutes for the indium to completely melt. The oven was then opened so that the test tube and stand could be removed and the impurities could be skimmed from the top of the molten metal. The oven was then closed and the crucible remained in the oven for a few minutes to re-melt. While the crucible remained in the oven, the area where the pour would occur was prepared. I put on welding gloves and placed a bucket of cool water near the test tube in case of an emergency spill. The stand was assembled and the glass test tube was placed securely inside. After roughly five minutes, the crucible was carefully removed and a small amount was poured into an aluminum tin to form the matching layer disc. The rest went into the glass test tube. The metal in the test tube was cooled indirectly by pouring cool water around the outside of the metal stand. Both pours were allowed to cool and harden overnight.

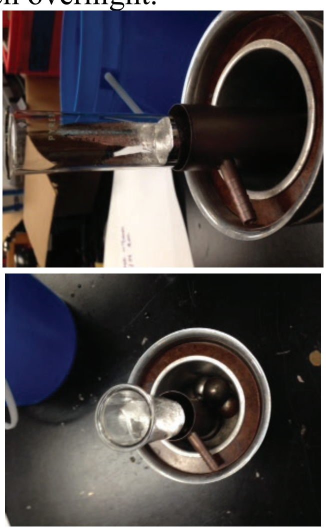

Fig 7. Test tube and stand immediately after pour (before wetting)

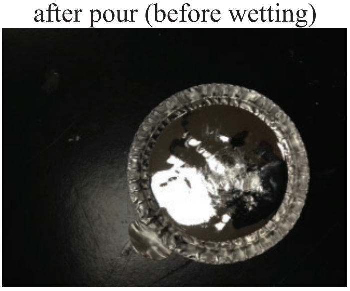

Fig 8. Indium disc immediately after pour

The disc was removed from the tin without issue (the indium did not adhere to aluminum). It was originally planned that the test tube would be safely shattered so that the indium rod may be removed, but when this was attempted, it was found that the indium had clung to the glass walls. The first solution to this problem was to use a lathe to remove the shattered glass, but the indium is so malleable that the movement of the machine altered the structure of the rod. The best solution to this issue was to sand the glass off of the rod. With a large belt sander it was possible to remove nearly all of the glass from around the rod. Since the glass caused small sparks to fly from the rod, it was very easy to tell when the majority of the glass has been removed.

Fig 9. Left: completed indium rod. Right: rod being sanded

During the pour, an air pocket formed down the middle of the indium rod that ended about halfway down. It was possible to remove this portion of the rod using a chop saw. Both ends were flattened and we were left with a 79 mm long indium rod.

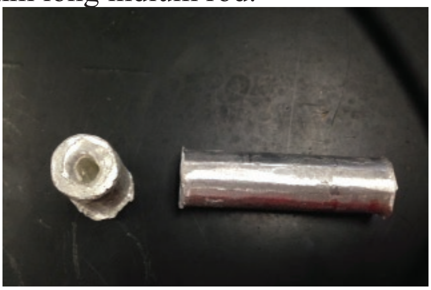

Fig 10. Indium rod with hollow area removed

When the disc was removed from the tin, it was apparent that surface tension had caused the top of the sample to be convex. A method had to be developed that would create a perfectly flat disc. The initial attempt to accomplish this was to use a sander, but this heated the indium up to nearly its melting point and caused deformation. This meant that by the time the indium was fully cooled, it needed to be as flat as possible. An attempt was made to flatten the disc by hand using an arbor press but this did not provide the amount of force that is needed to shape the indium, despite its malleability.

The sample was re-melted and re-poured according to the earlier procedure, but once the molten metal was in the tin, it was immediately placed onto a hot plate, another tin was set on top of it, and a 100 g weight held the upper tin flat. This method produced a very flat sample and was possible to repeat the process with larger tins to form larger discs.

Fig 11. Final technique for forming indium disc

XIII. Initial Tests of Indium as an Intermediate Layer

To confirm the hypothesis that placing an intermediate layer of material with acoustic impedance between that of the PZT transducer and the glass will increase the transmission of acoustic sound waves, a proper frequency had to be calculated and tested to determine whether or not it was possible.

The first measurement was made with only the glass, in order to see how much of the signal was passing through without implementing an intermediate layer. The signal was sent at 50 kHz.

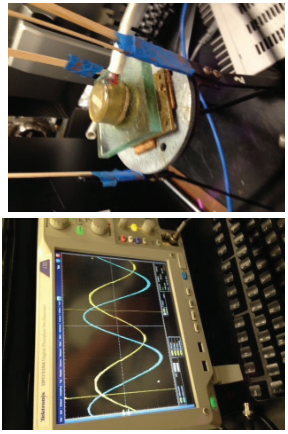

Fig 12. Left: Glass placed between signal and receiving piezos. Right: Sine wave representing these signals. The yellow wave is the signal sent by the upper piezo and the blue wave is the signal received by the lower piezo.

The second measurement was made after placing the 5.75mm disc of indium between the signal piezo and the glass.

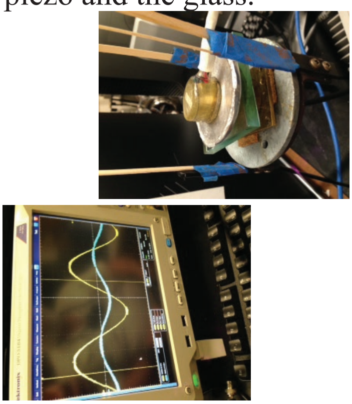

Fig 13. Left: Indium disc placed between the signal piezo and the glass. Right: Signal received by the lower piezo. It is significantly less than the signal seen without the indium layer.

XIV. Signal Cancelation

For a wave moving with speed V and a frequency f, the wavelength is:

$$\lambda = V/f$$

If the wave travels through a material of thickness equal to /4 then reflects and travels back to the first face, it will be 180° out of phase with the incoming wave. A portion of the wave going back into the original medium will then be partially cancelled, leading to a decrease in the overall reflection. The frequency at which this cancellation should happen for the shim of indium used in this measurement is as follows:

$$V/f = \lambda/4$$

$$f = 4V/\lambda$$

$$=(2.2 \text{ cm}/\mu\text{s})/(5.75\text{mm})(4)$$

$$=2.2/((4)(5.75))*10\text{^}6$$

$$=9.6\text{e}4\text{Hz}=96\text{kHz}$$

To determine the actual frequency at which cancellation occurs, a signal generator was used to sweep through a range of frequencies between 20 kHz and 110 kHz. At 103 kHz and 50 kHz, a 90 degree phase shift was seen, which suggests that, since 360 degrees is a full phase shift and 90 degrees is exactly ¼ of this, this is where our desired ¼ wavelength exists. The phase shift is seen at multiples of this frequency as well (1/2 wavelength, ¾ wavelength, ect.). The matching layer must be ¼ the width of the desired wavelength, which lives in this 103kHz frequency. The sound waves reflected off of the upper layer of the indium will travel a distance of 1/2 the wavelength when they are again reflected off of the lower layer. The reflected sound wave would then be 180 degrees out of phase with the original sound wave so they will be cancelled due to interference.

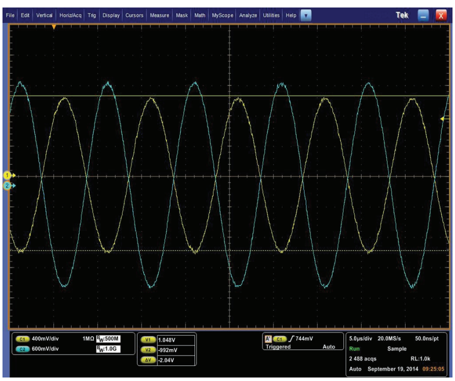

Fig 14. 90-degree phase shift seen at 103 kHz. This measurement was taken when the indium and glass, coupled together, were placed between the two piezos.

The fact that the phase shift is seen at several different frequencies suggests that our signal and the receiving piezos have different resonant frequencies, making the actual resonant frequency some average of these two values. It is promising to see the indium layer responding to a certain frequency in the expected manner.

XV. White Noise Testing

Another round of measurements were taken while the transducer was exposed to white noise caused by compressed air, simulating a range of all frequencies. This type of measurement is useful in our application due to a clear misinterpretation of the piezos resonant frequency. A transducer was placed on a stand and shot with compressed air—the signal was then captured and processed through MatLab as a waveform signal. From here, it was possible to create a Welch Power Spectrum that plots the signal with respect to acoustic power and frequency. This was then repeated with the glass only, and finally with the glass and the intermediate layer of indium.

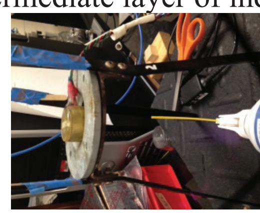

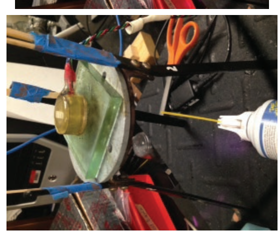

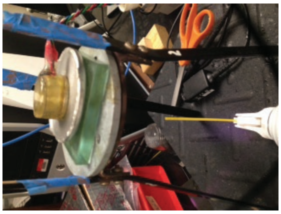

Fig 15. Each measurement was done by placing the piezo with it's various layers on a stand that is open at the bottom. They were each exposed to white noise via a can of compressed air.

After the waveforms were processed into a Welch Power Spectrum, they were each placed onto one graph with respect to power and frequency in order to compare signal power.

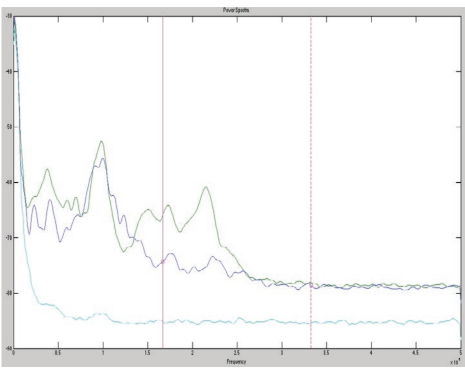

Fig 16. Welch Power Spectrum of white noise measurements. Green: Piezo only, Dark blue: Piezo and glass, Light blue: Piezo with glass and indium.

This spectra shows that the power of the signal received by the piezo is greatest (peaking when the frequency is ~100kHz) when there was no glass or indium between the compressed air and the transducer—as would be expected. There is some muffling done by the glass when it is introduced—another expected outcome. This can be seen at 100kHz, as the new peak is less than it was when there was nothing between the signal and the piezo. When the indium was introduced, the signal became clearly dampened as a result. There are no recognizable peaks, even at 100kHz.

XVI. Waveform Tests

In order to confirm these results, I took a closer look at each individual layer (piezos only, glass only, indium and glass) to see how it affected the sound wave. The measurement began by calculating a new t_0 by running a cycle with only the piezos. The time difference between the signal leaving one piezo and entering the other was 1.3 μs, shown in Figure 17.

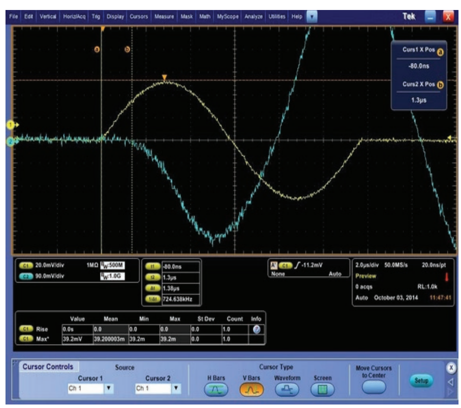

Fig 17. Piezo to piezo time delay. It is important to note that the received signal is amplified to nearly double to emitted signal.

Next, the glass was inserted between the piezos and another time difference was measured. With the glass, the overall delay of the system changed to 4.82 µs. Since the glass is 9.54 mm thick, we were able to calculate that the speed at which the signal to travel through the glass was 2690 m/s, which is rather inconsistent with our previous measurements. It can be seen in Figure 18 that the addition of the glass actually increased the overall signal transmission.

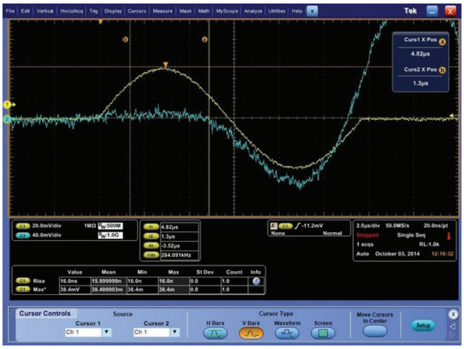

Fig 18. Signal when sent through the 9.54 mm thick piece of glass. It can be seen that the receive signal is much greater than the sent signal.

If the hypothesis is correct, when the indium is added to the system, we should see an increase in this transmission but, as can be seen in Figure 19, the signal is much less.

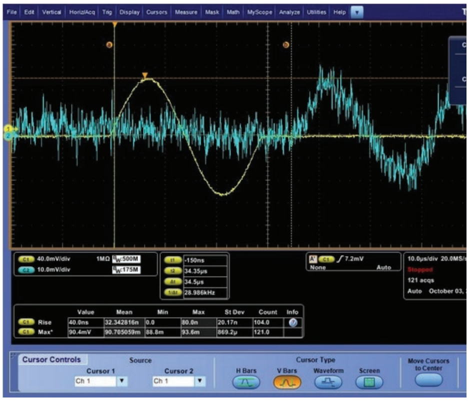

Fig 19. Completed system with glass and indium. The signal went from being more than double to about the same size as the signal pulse.

This measurement confirms what I have seen in all my previous tests. Indium, rather than increasing transmission, actually dampens signal.

XVII. Results

I have proven, through three different methods, that indium does not function as an intermediate layer for our acoustic transducers. More must be understood about the properties of indium to fully understand these results, but it can be seen throughout this paper that indium would function more efficiently as a backing layer for the transducers. This could improve transducer signals by containing the sound wave activity.

References

[1]Skycak, Justin P. “Designing a Matching Layer for Acoustic Sensors for the COUPP Dark Matter Detector”. Indiana University. 11 May 2013.

[2] F. Zwicky. (1937). On the masses of nebulae and of clusters of nebulae. The Astrophysical Journal. 86, 217-246

[3] Oort, Jan. “The Force Exerted by the Stellar System in the Direction Perpendicular to the Galactic Plane and Some Related Problems.”*Bulletin of the Astronomical Institutes of the Netherlands* 6 (1932): 248-87. *SAO/NASA ADS Astronomy Abstract Service*. Web. <http://adsabs.harvard.edu/abs/1932BAN.....6..249O>.

[4] Rubin, Vera. “Seeing dark matter in the Andromeda galaxy.” *Physics Today*. 59.12 (2006): 8-9. Print.

[5] V.C. Rubin, W.K. Jr. Ford, N. Thonnard. (1980. Rotational properties of 21 SC galaxies with a large range of luminosities and radii from NGC 4605 (R=4kpc) to UGV 2885 (R=122kpc). *The Astrophysical Journal, 86,* 471-487

[6] Schneider, Peter. “Detection of (dark) matter concentrations via weak gravitational lensing.” *Monthly Notices of the Royal Astronomical Society*. 283.3 (1996): 837-853. Print.

[7] Jedamzik, Karsten , and Maxim Pospelov. “Big Bang Nucleosynthesis and Particle Dark Matter.” *http://arxiv.org/abs/0906.2087v1* (2009): n.pag. *arXiv Database*. Web. 12 Jun 2013

[8] G. Bertone, D. Hooper, J. Silk. “Particle Dark Matter: Evidence, Candidates, and Constraints”. http://arxiv.org/abs/hep-ph/0404175v2 (2004): n.pag. *arXiv Database.* Web. Jun 26 2013.

[9] Feng, Jonathan L. “Dark Matter Candidates from Particle Physics and Methods of Detection.” *arXiv:1003.0904v2 [astro-ph.CO]*. (2010): 1-62. Web.

[10] L.D. Duffy, K. van Bibber. “Axions as Dark Matter Particles”. arXiv:0904.3346v1 [hep-ph] 21 Apr 2009: n.pag. *arXiv Database.* Web. June 26 2013.

[11] http://fermi.gsfc.nasa.gov/science/

[12] http://pamela.roma2.infn.it/index.php

[13] National Aeronautics and Space Administration. *NASA Administrator Statement on Alpha Magnetic Spectrometer.* Washington: 03 April 2013. Web. http://www.nasa.gov/home/hqnews/2013/apr/HQ_13-096_Bolden_AMS_Statement.html

[14] http://www.uslhc.us/LHC_Science/Questions_for_the_Universe/Dark_Matter

[15] http://www.snolab.ca/science/experiments/coupp

[16] W.J.Bolte, J.I.Collar, M.Crisler. "Development of Bubble Chambers With Enhanced Stability and Sensitivity to Low-Energy Nuclear Recoils". arXiv:astro-ph/0503398 v1. 17 Mar 2005: n.pag. *arXiv Database.* Web. June 26 2013.

[17] Aubin, F., Auger, M., & Genest, M. (2008). Discrimination of nuclear recoils from alpha particles with superheated liquids. *New Journal of Physics,* (10), 11-11. Retrieved from http://www.picassoexperiment.ca/dd_sitefiles/uploads/files/njp8_10_103017.pdf

[18] Behnke, E., Collar, J., & Cooper, P. (2008). Spin-Dependent WIMP Limits from a Bubble Chamber. *Science, 319*(5865), 3-3. Retrieved from http://www.sciencemag.org/content/319/5865/933.abstract?ijkey=IUVSv8kmcVidA&keytype=ref&siteid=sci

[19] Harris, O. (2014, April 14). COUPP60: for PNNL Collaboration Meeting. *PNNL Collaboration Meeting*. Talk conducted from PICO Collaboration.

20 http://hyperphysics.phy-astr.gsu.edu/hbase/sound/reflec.html

[21] Jaffe, B., W.R. Cook, and H. Jaffe. *Piezoelectric Ceramics*. New York, New York: Academic, 1971. Print.

[22] http://coupp-docdb.fnal.gov:8080/cgi-bin/RetrieveFile?docid=89;filename=acoustic_sensors%20Fermi_rev08.pdf;version=1

[23] Haynes, W. (Ed.). (2014). *CRC Handbook of Chemistry and Physics* (95th ed., p. 2704). CRC Press.

[24] https://www.nde-ed.org/GeneralResources/MaterialProperties/UT/ut_matlprop_metals.htm

Emily Mann is a senior and will graduate with a Bachelor of Science (B.S.) in Physics. This paper was written for research the student conducted under Dr. Ilan Levine in the Department of Physics and Astronomy.